PERGAMON

International Journal of Solids and Structures 38 (2001) 7261–7281

INTERNATIONAL JOURNAL OF SOLIDS and STRUCTURES

www.elsevier.com/locate/ijsolstr

A first order perturbation analysis of a non-ideal crack in a piezoelectric material

Zhenyu Huang, Zhen-Bang Kuang *

Department of Engineering Mechanics, School of Civil Engineering, Shanghai Jiaotong University, DongChuan Road 800#, Shanghai 200240, People's Republic of China

Received 3 September 1999

Abstract

In this paper a first order perturbation analysis is carried out on a symmetrically perturbed non-ideal crack for three kinds of electric boundary conditions, namely permeable, impermeable and conducting crack boundary condition. By using the extended Stroh formula, the two-domain problems are reduced to standard Riemann–Hilbert problems, and the singular integral equations of the internal electric field inside the permeable crack are solved. The stress and electric intensity factors (SEIFs) are determined to the first order of accuracy. The results indicate that for a symmetrically perturbed non-ideal crack the electro-mechanical loading at infinity does not affect the first order solution for the mode I intensity factor for general piezoelectric materials. The energy release rate and the SEIFs are determined by remote mechanical loads only and the perturbation effect on the SEIFs and energy release rate is small. The electric field distribution inside crack is constant for the zeroth order solution and quadratic for the first order solution, which is different from the constant electric field distribution for an ideal permeable crack. The internal electric concentration near the crack tip caused by the perturbation reveals that the dielectric inside the crack probably breaks down before the matrix does when the matrix is subjected to a not too high electro-mechanical load at infinity. The SEIFs and the energy release rate are also given for the non-ideal crack under the impermeable and conducting electric boundary condition respectively. For all three kinds of electric boundary conditions, the lateral stresses σ_{11}^{∞}, σ_{13}^{∞} have no contribution to the SEIFs to the first order of accuracy.

Keywords: Piezoelectric; Fracture; Perturbation analysis; Analytical continuation; Stroh formulism

1. Introduction

Owing to their intrinsic electro-elastic interaction, recently piezoceramics are widely used as actuators, sensors and transducers etc. Flaws, voids and microcracks inevitably exist in the manufacturing process of materials. When they are subjected to high operating loading or electric voltage, the reliability problem

* Corresponding author. Tel.: +86-21-54743067; fax: +86-21-62933021.
E-mail address: zbkuang@mail.sjtu.edu.cn (Z.-B. Kuang).

0020-7683/01/$ - see front matter
PII: S0020-7683(01)00004-X

arises in application of these materials to engineering devices. Many efforts have been devoted to the fracture mechanics of piezoelectric materials. Parton (1976) first investigated the fracture problem in piezoelectric materials and in his paper the crack was taken to be a permeable slit, i.e. the electric potential and normal component of the electric displacement were continuous across the crack surface. Deeg (1980), Pak (1990, 1992), Suo et al. (1992) addressed the plane and antiplane fracture problems of piezoelectric materials and obtained a closed form solution of the stress field and the electric displacement near the crack tip in terms of the impermeable electric boundary condition. Sosa (1991) used complex potential theory to investigate the elliptical void under the condition of plane deformation. Sosa and Khutoryansky (1996), Chung and Ting (1996), Gao and Fan (1999) further used an exact electric boundary condition to obtain the solution of an elliptical void in piezoelectrics. Chung and Ting (1996) also solved the inclusion problem in a piezoelectric media. Wang and Han (1999) and Gao and Wang (2000) solved an interface crack problem using the permeable crack boundary condition. Using the extended Stroh formalism and analytical continuation method, Shen and Kuang (1998) solved crack problems in a bi-piezothermoelastic media. In these papers the electric boundary condition is not fully identical with practical problems, because in reality there is a slight opening between two crack faces. McMeeking (1989) modeled the crack as a slender elliptic flaw with lower permittivity. He found that the approximation degree of the electric boundary condition depends on the parameter $(\epsilon_f/\epsilon_m)(a/b)$, where ϵ_f and ϵ_m are the permittivities of the media in the flaw and the matrix respectively and a and b are the semi-axes of the ellipse ($a > b$). Dunn (1994) pointed out that the impermeable assumption can lead to significant errors regarding the effects of the electric fields on crack propagation based on an energy release rate criterion. Hao and Shen (1994) considered the permeability of air in a crack gap and took the electric boundary condition as $D_2^+ = D_2^-$, $D_2^+(u_2^+ - u_2^-) = \epsilon_f(\phi^- - \phi^+)$. The electric displacement inside the crack was first assumed to be a constant, and then they solved the problem and proved that the assumption is reasonable. Zhang et al. (1998) adopted this assumption in their analysis for a permeable slender elliptic flaw. McMeeking (1999) employed finite element methods to simulate the experiment by Park and Sun (1995) for both permeable and impermeable electric boundary conditions. He also assumed a constant electric displacement field for the dielectric within the crack. However, the present model gives a non-homogeneous electric field distribution within the crack. Kuang (1979) and Wu (1982, 1994) solved a non-ideal crack problem for an isotropic material. Chen and Hsu (1997) further analyzed a non-ideal interface crack in an anisotropic media.

In this paper, we solve the problem of an infinite piezoelectric plate with a symmetrically perturbed non-ideal crack for three kinds of electric boundary conditions i.e. permeable (in Sections 3–6), impermeable and conducting boundary condition (Section 7). When the perturbation of the crack is small, we define the upper and lower surfaces of the crack as (Fig. 1) (In this paper notations $x_1 = x$, $x_2 = y$ will be adopted simultaneously.)

$$x_2 = \varepsilon Y_\pm(x_1) \quad \text{or} \quad y = \varepsilon Y_\pm(x), \quad |x_1| < a, \tag{1}$$

where

$$Y_+(x_1) - Y_-(x_1) \geqslant 0$$

and ε is a small parameter, $2a$ is the crack length. The subscripts "+" and "−" represent the value on the upper and lower crack surface respectively. At the ends of a non-ideal crack, we designate (Wu (1994) called it a regularly perturbed crack)

$$Y'_+(\pm a) - Y'_-(\pm a) = 0,$$

which ensures that crack tips are still mathematically sharp while the opposing crack faces are not in contact with each other. Generally, this situation coincides with most cracks in practical brittle materials.

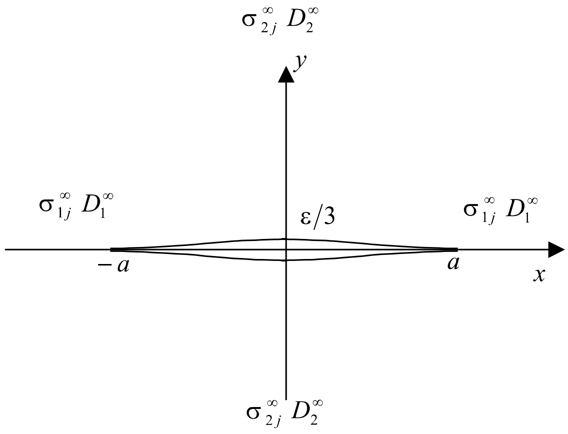

Fig. 1. The crack configuration and the remote loading condition.

2. Basic equations

In a fixed rectangular coordinate system (x_1, x_2, x_3), the constitutive equations for linear piezoelectrics of the second kind can be written as

$$\sigma_{ij} = c_{ijkl}u_{k,l} + e_{lij}\phi_{,l}, \qquad D_i = e_{ikl}u_{k,l} - \kappa_{il}\phi_{,l} \quad (i, j, k, l = 1, 2, 3), \tag{2}$$

where repeated Latin indices mean summation and a comma stands for partial differentiation. c_{ijkl} are the elastic stiffnesses under constant electric field, e_{ikl} the piezoelectric stress constants, and κ_{ij} the permittivity under constant strain field. σ_{ij}, u_j, D_i, E_i, and ϕ are stress, displacement, electric displacement, electric field and electric potential respectively. Here we only address general two-dimensional problems in the (x_1, x_2)-plane, i.e. all variables are constant along the x_3-axis. Following Suo (1993), Chung and Ting (1996) and Kuang and Ma (2000) the generalized displacement solution can be obtained by considering a linear combination of four complex analytical functions,

$$\mathbf{u} = \begin{Bmatrix} u_j \\ \phi \end{Bmatrix} = 2\mathrm{Re}\sum_{\alpha=1}^{4} \mathbf{a}_\alpha f_\alpha(z_\alpha), \qquad u_J = 2\mathrm{Re}\sum_{\alpha=1}^{4} a_{J\alpha} f_\alpha(z_\alpha). \tag{3}$$

The uppercase subscript ranges from 1 to 4, the lowercase subscript from 1 to 3. The generalized stress function, which is the resultant force on an arc, can be represented as,

$$\mathbf{\Phi}(z) = 2\mathrm{Re}\sum_{\alpha=1}^{4} \mathbf{b}_\alpha f_\alpha(z_\alpha), \qquad \Phi_J(z) = 2\mathrm{Re}\sum_{\alpha=1}^{4} b_{J\alpha} f_\alpha(z_\alpha), \tag{4}$$

where $z_\alpha = x_1 + p_\alpha x_2$ and Φ_j, $j = 1, 2, 3$ represents the component of resultant force and Φ_4 is the electric displacement flux on a curve. The eigenvalues p_α and the eigenvectors $\mathbf{a}_\alpha$ can be obtained from the following equations:

$$\left\lfloor \mathbf{Q} + \left(\mathbf{R} + \mathbf{R}^{\mathrm{T}}\right)p + \mathbf{T}p^2 \right\rfloor \mathbf{a} = \mathbf{0}, \tag{5}$$

where

$$\mathbf{Q} = \begin{bmatrix} \mathbf{Q}^E & \mathbf{e}_{11} \\ \mathbf{e}_{11}^{\mathrm{T}} & -\kappa_{11} \end{bmatrix}, \qquad \mathbf{R} = \begin{bmatrix} \mathbf{R}^E & \mathbf{e}_{21} \\ \mathbf{e}_{21}^{\mathrm{T}} & -\kappa_{12} \end{bmatrix}, \qquad \mathbf{T} = \begin{bmatrix} \mathbf{T}^E & \mathbf{e}_{22} \\ \mathbf{e}_{22}^{\mathrm{T}} & -\kappa_{22} \end{bmatrix},$$
$$Q_{ik}^E = c_{i1k1}, \quad R_{ik}^E = c_{i1k2}, \quad T_{ik}^E = c_{i2k2}, \quad (\mathbf{e}_{ij})_s = e_{ijs}, \tag{6}$$

and the eigenvectors $\mathbf{b}_\alpha$ can be obtained from the following relations,

$$\mathbf{b}_\alpha = \left(\mathbf{R}^{\mathrm{T}} + p_\alpha \mathbf{T}\right)\mathbf{a}_\alpha = -(\mathbf{Q} + p_\alpha \mathbf{R})\mathbf{a}_\alpha / p_\alpha. \tag{7}$$

From Eq. (7), the two equations can be recasted in the standard eigenrelation (Ting, 1996)

$$\begin{bmatrix} \mathbf{N}_1 & \mathbf{N}_2 \\ \mathbf{N}_3 & \mathbf{N}_1^{\mathrm{T}} \end{bmatrix} \begin{bmatrix} \mathbf{a} \\ \mathbf{b} \end{bmatrix} = p \begin{bmatrix} \mathbf{a} \\ \mathbf{b} \end{bmatrix},$$

$$\mathbf{N}_1 = -\mathbf{T}^{-1}\mathbf{R}^{\mathrm{T}}, \qquad \mathbf{N}_2 = \mathbf{T}^{-1}, \qquad \mathbf{N}_3 = \mathbf{R}\mathbf{T}^{-1}\mathbf{R}^{\mathrm{T}} - \mathbf{Q}. \tag{8}$$

Ting (1996) also shows

$$\mathbf{N}_3 = \begin{bmatrix} * & 0 & * & * \\ 0 & 0 & 0 & 0 \\ * & 0 & * & * \\ * & 0 & * & * \end{bmatrix}, \tag{9}$$

where $*$ stands for a possible non-zero value. The generalized Barnett–Lothe tensors are

$$\mathbf{S} = \mathrm{i}\left(2\mathbf{A}\mathbf{B}^{\mathrm{T}} - \mathbf{I}\right), \qquad \mathbf{L} = -2\mathrm{i}\mathbf{B}\mathbf{B}^{\mathrm{T}}. \tag{10}$$

The generalized stresses are as follows:

$$\Sigma_{2J}(z) = \begin{Bmatrix} \sigma_{2j} \\ D_2 \end{Bmatrix} = \Phi_{J,1} = 2\mathrm{Re}\left[\sum_{\alpha=1}^{4} b_{J\alpha} f_\alpha'(z_\alpha)\right],$$
$$\Sigma_{1J}(z) = \begin{Bmatrix} \sigma_{1j} \\ D_1 \end{Bmatrix} = -\Phi_{J,2} = -2\mathrm{Re}\left[\sum_{\alpha=1}^{4} b_{J\alpha} p_\alpha f_\alpha'(z_\alpha)\right]. \tag{11}$$

For stable materials eigenvalues cannot be real (Suo et al., 1992; Ting, 1996). Note in this paper that implicit summation convention is used only for Latin indices, while for Greek indices we write the summation symbol explicitly.

The electric potential of the isotropic dielectric inside the crack can be expressed as a real part of a complex analytical function $g(z)$ in z-plane,

$$\phi^{\mathrm{c}}(x, y) = g(z) + \overline{g(z)} = 2\mathrm{Re}[g(z)], \tag{12}$$

where $z = x + \mathrm{i}y$. The overbar indicates a conjugate value and the superscript c represents the field inside the crack. Thus we have the electric field and electric displacement inside the crack,

$$E_1^{\mathrm{c}}(x, y) = -2\mathrm{Re}\left[g'(z)\right], \qquad D_1^{\mathrm{c}}(x, y) = -2\epsilon_{\mathrm{f}}\mathrm{Re}\left[g'(z)\right],$$
$$E_2^{\mathrm{c}}(x, y) = 2\mathrm{Im}\left[g'(z)\right], \qquad D_2^{\mathrm{c}}(x, y) = 2\epsilon_{\mathrm{f}}\mathrm{Im}\left[g'(z)\right], \tag{13}$$

where ϵ_{f} is the permittivity of the dielectric inside the crack.

3. Perturbation analysis for the permeable non-ideal crack

We consider an infinite piezoelectric media with a non-ideal centered crack, which is traction-free on its crack faces and subjected to a mechanical loading σ_{22}^{∞}, σ_{21}^{∞}, σ_{23}^{∞}, σ_{11}^{∞}, σ_{13}^{∞} and an electric loading D_1^{∞}, D_2^{∞} at infinity. By means of perturbation theory, we can expand the complex function $f_\alpha(z_\alpha)$ in powers of ε,

$$f_\alpha(z_\alpha) = f_\alpha(z_\alpha;\varepsilon) = \sum_{n=0}^{\infty}\frac{\varepsilon^n}{n!}f_{\alpha n}(z_\alpha) = f_{\alpha 0}(z_\alpha) + \varepsilon f_{\alpha 1}(z_\alpha) + \cdots \tag{14}$$

We direct our focus only to the first order solution so the higher order term will be ignored. We express the point on the crack face with $*$,

$$z^* = x + \mathrm{i}\varepsilon Y_\pm(x), \qquad z_\alpha^* = x + \varepsilon p_\alpha Y_\pm(x), \quad |x| \leqslant a. \tag{15}$$

Therefore the function $f_\alpha(z_\alpha^*)$ can be expanded as follows,

$$f_{\alpha n}\left(z_\alpha^*\right) = \sum_{n=0}^{\infty}\frac{\varepsilon^n}{n!}f_{\alpha n}\left(z_\alpha^*\right) = f_{\alpha n}^{\pm}(x) + \varepsilon p_\alpha Y_\pm(x) f_{\alpha n}^{\prime\pm}(x) + O\left(\varepsilon^2\right), \tag{16}$$

where $f_{\alpha n}^{\pm}(x)$ stand for values on the crack surfaces at $z^* = x + \varepsilon p_\alpha Y_\pm(x)$ respectively.

We can expand $g(z)$, $g_n(z^*)$ in the same manner,

$$\begin{cases} g(z) = g_0(z) + \varepsilon g_1(z) + O(\varepsilon^2), \\ g_n(z^*) = g_n(x) + i\varepsilon Y_\pm(x) g_n'(x) + O(\varepsilon^2). \end{cases} \tag{17}$$

The traction free boundary condition, the continuity of the electric displacement in the normal direction at the boundary and the continuity of electric field in the tangential direction or the continuity of electric potential at the boundary curve require

$$\begin{cases} 2\mathrm{Re}\sum_\alpha b_{j\alpha} f_\alpha\left(z_\alpha^*\right) = 0, \\ 2\mathrm{Re}\sum_\alpha b_{4\alpha} f_\alpha\left(z_\alpha^*\right) = 2\epsilon_{\mathrm{f}}\mathrm{Im}[g(z^*)], \\ 2\mathrm{Re}\sum_\alpha a_{4\alpha} f_\alpha\left(z_\alpha^*\right) = 2\mathrm{Re}[g(z^*)]. \end{cases} \tag{18}$$

Hence the boundary condition to the first order of accuracy for ε^0, ε^1 can be expressed respectively as follows,

$$\begin{cases} 2\mathrm{Re}\sum_\alpha b_{j\alpha} f_{\alpha 0}^{\pm}(x) = 0, \\ 2\mathrm{Re}\sum_\alpha b_{4\alpha} f_{\alpha 0}^{\pm}(x) = 2\epsilon_{\mathrm{f}}\mathrm{Im}[g_0(x)], \quad x \in L, \\ 2\mathrm{Re}\sum_\alpha a_{4\alpha} f_{\alpha 0}^{\pm}(x) = 2\mathrm{Re}[g_0(x)], \end{cases} \tag{19}$$

$$\begin{cases} 2\mathrm{Re}\sum_\alpha b_{j\alpha}\left[p_\alpha Y_\pm(x) f_{\alpha 0}^{\prime\pm}(x) + f_{\alpha 1}^{\pm}(x)\right] = 0, \\ 2\mathrm{Re}\sum_\alpha b_{4\alpha}\left[p_\alpha Y_\pm(x) f_{\alpha 0}^{\prime\pm}(x) + f_{\alpha 1}^{\pm}(x)\right] = 2\epsilon_{\mathrm{f}}\mathrm{Im}\left[\mathrm{i}Y_\pm(x) g_0'(x) + g_1(x)\right], \quad x \in L, \\ 2\mathrm{Re}\sum_\alpha a_{4\alpha}\left[p_\alpha Y_\pm(x) f_{\alpha 0}^{\prime\pm}(x) + f_{\alpha 1}^{\pm}(x)\right] = 2\mathrm{Re}\left[\mathrm{i}Y_\pm(x) g_0'(x) + g_1(x)\right]. \end{cases} \tag{20}$$

L is the line in the interval of $(-a, a)$. It is worth noticing that in Eq. (20) only the lateral component of generalized stresses of the zeroth order, i.e. $\Sigma_{1J}^{(0)}$ in Eq. (11), can affect the first order solution. The remote stress and electric boundary conditions are

$$\begin{cases} \Sigma_{2J}^{\infty} = \{\Sigma_{2J}(z)\}_{z\to\infty} = \begin{Bmatrix} \sigma_{2j}^{\infty} \\ D_2^{\infty} \end{Bmatrix} = 2\mathrm{Re}\left[\sum_{\alpha=1}^{4} b_{J\alpha} f_\alpha'(z_a)\right]_{z_\alpha\to\infty}, \\ \Sigma_{1J}^{\infty} = \{\Sigma_{1J}(z)\}_{z\to\infty} = \begin{Bmatrix} \sigma_{1j}^{\infty} \\ D_1^{\infty} \end{Bmatrix} = -2\mathrm{Re}\left[\sum_{\alpha=1}^{4} b_{J\alpha} p_\alpha f_\alpha'(z_a)\right]_{z_\alpha\to\infty}. \end{cases} \tag{21}$$

Noticing Eqs. (16) and (21) can be rewritten in the following form,

$$\begin{cases} \Sigma_{2J}^{\infty} = 2\mathrm{Re}\left[\sum_{\alpha=1}^{4} b_{J\alpha} f_{\alpha 0}'(z_a)\right]_{z_\alpha\to\infty}, & \Sigma_{1J}^{\infty} = -2\mathrm{Re}\left[\sum_{\alpha=1}^{4} b_{J\alpha} p_\alpha f_{\alpha 0}'(z_a)\right]_{z_\alpha\to\infty}, \\ 0 = 2\mathrm{Re}\left[\sum_{\alpha=1}^{4} b_{J\alpha} f_{\alpha 1}'(z_a)\right]_{z_\alpha\to\infty}, & 0 = -2\mathrm{Re}\left[\sum_{\alpha=1}^{4} b_{J\alpha} p_\alpha f_{\alpha 1}'(z_a)\right]_{z_\alpha\to\infty}. \end{cases} \tag{22}$$

The single-value condition of displacement requires (Suo et al., 1992; Wang and Han, 1999)

$$\begin{aligned} &\int_{-a}^{a}\left[\sum_{\alpha=1}^{4} b_{J\alpha} f_{\alpha 0}'^{+}(x) - \sum_{\alpha=1}^{4} b_{J\alpha} f_{\alpha 0}'^{-}(x)\right] = 0, \\ &\int_{-a}^{a}\left[\sum_{\alpha=1}^{4} b_{J\alpha} f_{\alpha 1}'^{+}(x) - \sum_{\alpha=1}^{4} b_{J\alpha} f_{\alpha 1}'^{-}(x)\right] = 0. \end{aligned} \tag{23}$$

Now the controlling equations for the permeable electric boundary value problem to the first order of accuracy are complete. In Sections 4 and 5, efforts will be mainly made to solve the boundary problems for the zeroth order and the first order solution respectively. Section 6 concerns about the energy release rate for the permeable non-ideal crack.

4. The solution of the order of ε^0

First we solve the zeroth order solution, viz. the solution for a permeable ideal crack. We rewrite Eq. (19) in a compact form,

$$\begin{cases} 2\mathrm{Re}\sum_\alpha b_{J\alpha} f_{\alpha 0}^{\pm}(x) = T_{J0}, \\ 2\mathrm{Re}\sum_\alpha a_{4\alpha} f_{\alpha 0}^{\pm}(x) = 2\mathrm{Re}[g_0(x)], \end{cases} \quad x \in L, \tag{24}$$

where

$$T_{J0}(x) = \{0,\ 0,\ 0,\ 2\epsilon_{\mathrm{f}}\mathrm{Im}[g_0(x)]\}. \tag{25}$$

From the first term of Eq. (24) we have,

$$\begin{cases} \sum_\alpha \left(b_{J\alpha} f_{\alpha 0}^{+}(x) - \bar{b}_{J\alpha}\bar{f}_{\alpha 0}^{+}(x)\right) - \sum_\alpha \left(b_{J\alpha} f_{\alpha 0}^{-}(x) - \bar{b}_{J\alpha}\bar{f}_{\alpha 0}^{-}(x)\right) = 0, \\ \sum_\alpha \left(b_{J\alpha} f_{\alpha 0}^{+}(x) + \bar{b}_{J\alpha}\bar{f}_{\alpha 0}^{+}(x)\right) + \sum_\alpha \left(b_{J\alpha} f_{\alpha 0}^{-}(x) + \bar{b}_{J\alpha}\bar{f}_{\alpha 0}^{-}(x)\right) = 2T_{J0}(x). \end{cases} \tag{26}$$

It is obvious that Eq. (26) can be solved as a non-homogeneous Riemann–Hilbert problem. Since the remote loading is constant, from the first term of Eq. (26), one reaches,

$$\sum_\alpha \left(b_{J\alpha} f_{\alpha 0}(z) - \bar{b}_{J\alpha}\bar{f}_{\alpha 0}(z)\right) = \mathrm{i}C_{0J}z, \tag{27}$$

where C_{0J} is the component of a real vector to be determined from remote boundary condition. Note that in the above equation a subscript α for z is dropped and a replacement should be made once the solution $f_{\alpha 0}(z)$ obtained. From the second term of Eq. (26), a finite solution at the crack ends is

$$\sum_\alpha \left(b_{J\alpha} f_{\alpha 0}(z) + \bar{b}_{J\alpha}\bar{f}_{\alpha 0}(z)\right) = \frac{X(z)}{2\pi \mathrm{i}}\int_L \frac{2T_{J0}(t)}{X^{+}(t)(t-z)}\mathrm{d}t + C_{1J}X(z), \tag{28}$$

where $X(z) = (z^2 - a^2)^{1/2}$ and C_{1J} is the component of a real vector. The branch cut of $X(z)$ is taken as z when $z \to \infty$, so $X^{\pm}(x) = \pm \mathrm{i}(a^2 - x^2)^{1/2}$ for $|x| < a$. Hence the complex function $f_{\alpha 0}(z_\alpha)$ given by

$$f_{\alpha 0}(z_\alpha) = \frac{b_{\alpha J}^{-1}X(z_\alpha)}{2\pi \mathrm{i}}\int_L \frac{T_{J0}(t)}{(t-z_\alpha)X^{+}(t)}\mathrm{d}t + \frac{1}{2}b_{\alpha J}^{-1}(C_{1J}X(z_\alpha) + \mathrm{i}C_{0J}z_\alpha) \tag{29}$$

is an analytical function in z_α plane (Suo, 1990; Kuang and Ma, 2000), where $b_{\alpha J}^{-1}$ is the element of $[b_{J\alpha}]^{-1}$. In Eq. (29), the first term containing an integral at the right-hand side is finite and its derivative is zero when $z_\alpha \to \infty$. So invoking the remote field boundary condition, one gets

$$\begin{cases} C_{1J} = \Sigma_{2J}^\infty, \\ C_{0K}\mathrm{Im}\left[\sum_\alpha b_{J\alpha}p_\alpha b_{\alpha K}^{-1}\right] - C_{1K}\mathrm{Re}\left[\sum_\alpha b_{J\alpha}p_\alpha b_{\alpha K}^{-1}\right] = \Sigma_{1J}^\infty. \end{cases} \tag{30}$$

In Eq. (30), since $\Sigma_{21}^\infty = \Sigma_{12}^\infty$, there are eight undetermined constants for seven independent equations. Ting (1996) proved the following relation

$$\mathbf{BPB}^{-1} = \left(\mathbf{N}_1^\mathrm{T} - \mathbf{N}_3\mathbf{SL}^{-1}\right) - \mathrm{i}\mathbf{N}_3\mathbf{L}^{-1}, \tag{31}$$

where $\mathbf{P} = \mathrm{diag}[p_1, p_2, p_3]$ for anisotropic materials. It is easy to prove that this relation also holds for piezoelectric materials. Noticing Eq. (9), we have

$$\mathrm{Im}\left[\sum_\alpha b_{2\alpha}p_\alpha b_{\alpha K}^{-1}\right] = 0. \tag{32}$$

So not losing generality, we set $C_{02} = 0$. To get the other values of C_{0J}, a simple numerical procedure is necessary. For Eq. (29), the single-value condition of displacement is satisfied. Using the second term of Eq. (24), the unknown function $T_{40}(x)$ can be determined from a singular integral equation. From the second term of Eq. (24), we have

$$\sum_\alpha a_{4\alpha}\left(f_{\alpha 0}^+(x) - f_{\alpha 0}^-(x)\right) = \sum_\alpha \overline{a}_{4\alpha}\left(\overline{f}_{\alpha 0}^+(x) - \overline{f}_{\alpha 0}^-(x)\right). \tag{33}$$

Substituting Eq. (29) into Eq. (33) gives,

$$\sum_\alpha\left[\frac{a_{4\alpha}b_{\alpha J}^{-1} - \overline{a}_{4\alpha}\overline{b}_{\alpha J}^{-1}}{\pi \mathrm{i}}\int_L \frac{T_{J0}(t)}{(t-x)X^+(t)}\mathrm{d}t + \left(a_{4\alpha}b_{\alpha J}^{-1} - \overline{a}_{4\alpha}\overline{b}_{\alpha J}^{-1}\right)C_{1J}\right] = 0. \tag{34}$$

We define $M_{KJ} = \sum_\alpha a_{K\alpha}b_{\alpha J}^{-1}$, $H_{KJ} = \mathrm{i}(M_{KJ} - \overline{M}_{KJ})$. H_{KJ} is a real symmetric matrix (Suo et al., 1992). Considering Eq. (25), the integral equation for $T_{40}(x)$ can be given by

$$\left(M_{4J} - \overline{M}_{4J}\right)C_{1J}\pi\mathrm{i} + \left(M_{44} - \overline{M}_{44}\right)\int_L \frac{T_{40}(t)}{(t-x)X^+(t)}\mathrm{d}t = 0. \tag{35}$$

With the knowledge of singular integral equations in Muskhelishevili (1953, 1975), we find

$$T_{40}(x) = \frac{M_{4J} - \overline{M}_{4J}}{M_{44} - \overline{M}_{44}}\Sigma_{2J}^\infty x = Cx, \tag{36}$$

where $C = H_{4J}\Sigma_{2J}^\infty / H_{44}$. Some singular integrals are listed in the Appendix A for references. With the availability of $T_{40}(x)$ and Eq. (29), the zeroth order solution can be obtained for the field both outside and inside the crack, which was also discussed by Wang and Han (1999) and Gao and Fan (1999)

$$f_{\alpha 0}(z_\alpha) = \tfrac{1}{2}[U_\alpha X(z_\alpha) + V_\alpha z_\alpha], \tag{37}$$

where

$$\begin{cases} U_\alpha = b_{\alpha J}^{-1}\Sigma_{2J}^\infty - b_{\alpha 4}^{-1}C = \left(b_{\alpha j}^{-1} - b_{\alpha 4}^{-1}\frac{H_{4j}}{H_{44}}\right)\Sigma_{2j}^\infty, \\ V_\alpha = \mathrm{i}b_{\alpha J}^{-1}C_{0J} + b_{\alpha 4}^{-1}C. \end{cases} \tag{38}$$

It is obvious in Eq. (38) that U_α depends only on the mechanical load at infinity and is independent of the lateral stress component σ_{11}^∞, σ_{13}^∞ and the electric loading at infinity. Combining the second term of Eq. (24) with Eq. (37), one gets

$$2\mathrm{Re}[g_0(x)] = \mathrm{Re}[\mathrm{i}M_{4J}C_{0J} + M_{44}C]x. \tag{39}$$

Hence the zeroth order electric field distribution within the crack on the x-axis is given by

$$\begin{cases} E_2^{(0)\mathrm{c}}(x,0) = H_{4J}\Sigma_{2J}^{\infty}/(H_{44}\epsilon_\mathrm{f}) = D_2^{\infty}/\epsilon_\mathrm{f} + H_{4j}\Sigma_{2j}^{\infty}/H_{44}, \\ E_1^{(0)\mathrm{c}}(x,0) = -\mathrm{Re}[\mathrm{i}M_{4J}C_{0J} + M_{44}C] = E_1^{\infty} + \mathrm{Re}\left[\sum_{\alpha=1}^{4} a_{4\alpha}U_\alpha\right]. \end{cases} \tag{40}$$

It can be seen that the zeroth electric field inside the crack is constant which can be regarded as a special kind of elliptical inhomogeneity whose field distribution is constant when the matrix subjected to constant loading condition at infinity as indicated by Wang (1992) and Sosa and Khutoryansky (1996). When there is no mechanical loading at infinity, the electric field inside the crack is (Gao and Fan, 1999)

$$E_1^{(0)\mathrm{c}}(x,0) = E_1^{\infty}, \qquad E_2^{(0)\mathrm{c}}(x,0) = D_2^{\infty}/\epsilon_\mathrm{f},$$

which indicates that for the zeroth order solution under the permeable condition the crack cannot disturb the electric field distribution in the matrix. For simplicity, we designate $\Theta_\alpha = \cos\theta + p_\alpha\sin\theta$. Based on the solution (37), the zeroth order solution for generalized stress $\Sigma_{2J}^{(0)}(r,\theta)$ is,

$$\Sigma_{2J}^{(0)}(r,\theta) = \frac{\sqrt{a}}{\sqrt{2r}}\mathrm{Re}\left[\sum_\alpha b_{J\alpha}U_\alpha\frac{1}{\sqrt{\Theta_\alpha}}\right] + \delta_{4J}C + O\left(\sqrt{r}\right), \tag{41}$$

where (r,θ) is the polar coordinate with its origin located at the right tip and δ_{4J} is Kronecker delta. It can be seen that the remote electric loading comes into influence in the non-singular part in front of the crack tip. The singular terms of Eq. (41) on the x-axis in front of the right crack tip is

$$\Sigma_{2J\,\mathrm{singular}}^{(0)}(r,0) = \frac{\sqrt{a}}{\sqrt{2r}}\left[\Sigma_{2J}^{\infty} - \delta_{4J}\frac{H_{4K}}{H_{44}}\Sigma_{2K}^{\infty}\right]. \tag{42}$$

By Irwin's nomenclature (Irwin, 1957), the stress and electric intensity factors (SEIFs) can be written as

$$\begin{cases} K_1^{(0)} = \sqrt{\pi a}\sigma_{22}^{\infty}, \qquad K_2^{(0)} = \sqrt{\pi a}\sigma_{21}^{\infty}, \\ K_3^{(0)} = \sqrt{\pi a}\sigma_{23}^{\infty}, \qquad K_4^{(0)} = -\sqrt{\pi a}\sigma_{2j}^{\infty}H_{4j}/H_{44}. \end{cases} \tag{43}$$

The above result suggests that stress intensity factors (SIFs) only depend on the remote stress loading and the crack length. The electric intensity factor (EIF) is independent of the remote electric loading and the dielectric property inside the crack. Pure mechanical loads can also cause EIF. The result is identical with Wang and Han (1999) and Gao and Fan (1999). With Eq. (37), the generalized displacement is

$$u_J^{(0)}(r,\theta) = \mathrm{Re}\left[\sum_{\alpha=1}^{4} a_{J\alpha}\left(U_\alpha\sqrt{2ar\Theta_\alpha} + V_\alpha a + V_\alpha r\Theta_\alpha\right)\right] + O\left(r^{3/2}\right). \tag{44}$$

We reiterate that the zeroth order solution, i.e. the solution for a permeable ideal crack, the remote field electric load cannot effect the SEIFs. This conclusion applies to various types of small perturbed crack problems.

5. The solution to the order of ε^1

In this section, the solution procedure is the same as that in Section 4. However, it is quite difficult to get a solution for a generally perturbed crack face. In the following, even a specific symmetric perturbed crack configuration causes great difficulty in solving the first order solution. From Eq. (20), for the first order problem the boundary condition can be recast as,

$$\begin{cases} 2\mathrm{Re}\sum_\alpha b_{J\alpha} f_{\alpha 1}^{\pm}(x) = T_{J1}^{\pm}(x), \\ 2\mathrm{Re}\sum_\alpha a_{4\alpha}\left[p_\alpha Y_\pm(x) f_{\alpha 0}'^{\pm}(x) + f_{\alpha 1}^{\pm}(x)\right] = 2\mathrm{Re}\left[\mathrm{i}Y_\pm(x) g_0'(x) + g_1(x)\right], \end{cases} \quad x \in L, \tag{45}$$

where

$$T_{J1}^{\pm}(x) = -2Y_\pm(x)\mathrm{Re}\left[\sum_\alpha b_{J\alpha} p_\alpha f_{\alpha 0}'^{\pm}(x)\right] + 2\delta_{4J}\epsilon_{\mathrm{f}}\mathrm{Im}\left[\mathrm{i}Y_\pm(x) g_0'(x) + g_1(x)\right]. \tag{46}$$

From the first term of Eq. (45) we have,

$$\begin{cases} \sum_\alpha \left(b_{J\alpha} f_{\alpha 1}^{+}(x) - \overline{b}_{J\alpha}\overline{f}_{\alpha 1}^{+}(x)\right) - \sum_\alpha \left(b_{J\alpha} f_{\alpha 1}^{-}(x) - \overline{b}_{J\alpha}\overline{f}_{\alpha 1}^{-}(x)\right) = T_{J1}^{+}(x) - T_{J1}^{-}(x), \\ \sum_\alpha \left(b_{J\alpha} f_{\alpha 1}^{+}(x) + \overline{b}_{J\alpha}\overline{f}_{\alpha 1}^{+}(x)\right) + \sum_\alpha \left(b_{J\alpha} f_{\alpha 1}^{-}(x) + \overline{b}_{J\alpha}\overline{f}_{\alpha 1}^{-}(x)\right) = T_{J1}^{+}(x) + T_{J1}^{-}(x). \end{cases} \tag{47}$$

If the materials are the same in Chen and Hsu (1997) and the electric component is neglected, the above terms of Eq. (47) are identical with the first order controlling Eqs. (51) and (52) in their paper. Since the remote boundary condition is not affected by the perturbation of crack faces (see Eq. (22)), $f_{\alpha 1}(z_\alpha)$ tends to be zero when z_α goes to infinite. Hence, we get

$$\begin{cases} \sum_\alpha \left(b_{J\alpha} f_{\alpha 1}(z) - \overline{b}_{J\alpha}\overline{f}_{\alpha 1}(z)\right) = \frac{1}{2\pi\mathrm{i}}\int_L \frac{T_{J1}^{+}(t) - T_{J1}^{-}(t)}{t-z}\mathrm{d}t, \\ \sum_\alpha \left(b_{J\alpha} f_{\alpha 1}(z) + \overline{b}_{J\alpha}\overline{f}_{\alpha 1}(z)\right) = \frac{X(z)}{2\pi\mathrm{i}}\int_L \frac{\left(T_{J1}^{+}(t) + T_{J1}^{-}(t)\right)}{(t-z)X^{+}(t)}\mathrm{d}t. \end{cases} \tag{48}$$

So, the first order solution can be given by

$$f_{\alpha 1}(z_\alpha) = \frac{1}{2}b_{\alpha J}^{-1}\left[\frac{X(z_\alpha)}{2\pi\mathrm{i}}\int_L \frac{\left(T_{J1}^{+}(t) + T_{J1}^{-}(t)\right)}{(t-z_\alpha)X^{+}(t)}\mathrm{d}t + \frac{1}{2\pi\mathrm{i}}\int_L \frac{T_{J1}^{+}(t) - T_{J1}^{-}(t)}{t - z_\alpha}\mathrm{d}t\right]. \tag{49}$$

In this paper we focus our attention mainly on the influence of electric field on the SEIFs. In order to make the solution tractable rather than in a prolix integral form, we confine the perturbed crack face configuration to a specific case,

$$Y_\pm(x) = \pm Y(x) = \pm\left(a^2 - x^2\right)^{3/2}/3a^2. \tag{50}$$

Substituting the zeroth order solution into Eq. (46), we write

$$\begin{cases} T_{J1}^{+}(x) + T_{J1}^{-}(x) = 2\mathrm{Re}\left[\sum_\alpha \mathrm{i}b_{J\alpha}p_\alpha U_\alpha\right]\frac{xY(x)}{\sqrt{a^2-x^2}} + 4\delta_{4J}\epsilon_{\mathrm{f}}\mathrm{Im}[g_1(x)], \\ T_{J1}^{+}(x) - T_{J1}^{-}(x) = -2\left(\mathrm{Re}\left[\sum_\alpha b_{J\alpha}p_\alpha V_\alpha\right] + \delta_{4J}\epsilon_{\mathrm{f}}E_1^{(0)\mathrm{c}}\right)Y(x). \end{cases} \tag{51}$$

Invoking the singular integral equations listed in the Appendix A and substituting Eq. (51) into Eq. (49), it is not difficult to get

$$\begin{aligned} f_{\beta 1}(z_\beta) = \frac{b_{\beta J}^{-1}}{a^2}\Bigg\{&\frac{a^2\delta_{4J}\epsilon_{\mathrm{f}}X(z_\beta)}{\pi\mathrm{i}}\int_L \frac{\mathrm{Im}[g_1(t)]}{(t-z_\beta)X^{+}(t)}\mathrm{d}t - \frac{1}{6}\mathrm{Re}\left[\sum_\alpha \mathrm{i}b_{J\alpha}p_\alpha U_\alpha\right]X(z_\beta)\left(z_\beta X(z_\beta) - z_\beta^2 + \frac{a^2}{2}\right) \\ &+ \frac{\mathrm{i}}{6}\left(\mathrm{Re}\left[\sum_\alpha b_{J\alpha}p_\alpha V_\alpha\right] + \epsilon_{\mathrm{f}}\delta_{4J}E_1^{(0)\mathrm{c}}\right)\left(a^2X(z_\beta) - \frac{3}{2}a^2z_\beta + z_\beta^3 - z_\beta^2X(z_\beta)\right)\Bigg\}. \end{aligned} \tag{52}$$

From the second term of Eq. (45) we get

$$2\mathrm{Re}\left[\sum_\alpha a_{4\alpha}\left(f_{\alpha 1}^{+}(x) - f_{\alpha 1}^{-}(x)\right)\right] + 2\left(\mathrm{Re}\left[\sum_\alpha a_{4\alpha}p_\alpha V_\alpha\right] + E_2^{(0)\mathrm{c}}\right)Y(x) = 0. \tag{53}$$

Considering Eq. (52), the singular integral equation for $\mathrm{Im}[g_1(x)]$ can be obtained,

$$A_1 \int_L \frac{\mathrm{Im}[g_1(t)]}{(t-x)X^+(t)}\mathrm{d}t - \frac{1}{3a^2}(A_2+A_3)x^2 + \frac{1}{3}\left(\frac{A_2}{2}+A_3\right) = 0, \tag{54}$$

where

$$\begin{aligned} A_1 &= -\frac{2H_{44}\epsilon_{\mathrm{f}}}{\pi}, \qquad A_2 = \mathrm{i}H_{4J}\mathrm{Re}\left[\sum_\alpha \mathrm{i}b_{J\alpha}p_\alpha U_\alpha\right], \\ A_3 &= \mathrm{i}\left\{2\mathrm{Re}[M_{4J}]\left(\epsilon_{\mathrm{f}}\delta_{4J}E_1^{(0)\mathrm{c}} + \mathrm{Re}\left[\sum_\alpha b_{J\alpha}p_\alpha V_\alpha\right]\right) - 2\left(\mathrm{Re}\left[\sum_\alpha a_{4\alpha}p_\alpha V_\alpha\right] + E_2^{(0)\mathrm{c}}\right)\right\}. \end{aligned} \tag{55}$$

A_1, A_2, A_3 are constants, which depend on materials properties of the matrix and the dielectric inside the crack and the remote electro-mechanical loading. The solution to the above singular integral equation is

$$\mathrm{Im}[g_1(x)] = \frac{-1}{\pi \mathrm{i}A_1}\left[\frac{1}{3a^2}(A_2+A_3)x^3 - x\left(\frac{A_3}{2}+\frac{A_2}{3}\right)\right]. \tag{56}$$

Then substitution of Eq. (56) into Eq. (52) yields

$$\begin{aligned} f_{\beta 1}(z_\beta) = \frac{b_{\beta J}^{-1}}{a^2}\Bigg\{ &-\frac{X(z_\beta)\epsilon_{\mathrm{f}}\delta_{4J}}{\pi \mathrm{i}A_1}\left[\frac{1}{3}(A_2+A_3)\left(\frac{z_\beta^3}{X(z_\beta)} - z_\beta^2 - \frac{a^2}{2}\right) - a^2\left(\frac{A_2}{3}+\frac{A_3}{2}\right)\left(\frac{z_\beta}{X(z_\beta)}-1\right)\right] \\ &-\frac{1}{6}\mathrm{Re}\left[\sum_\alpha \mathrm{i}b_{J\alpha}p_\alpha U_\alpha\right]X(z_\beta)\left(z_\beta X(z_\beta) - z_\beta^2 + \frac{a^2}{2}\right) \\ &+\frac{\mathrm{i}}{6}\left(\mathrm{Re}\left[\sum_\alpha b_{J\alpha}p_\alpha V_\alpha\right] + \epsilon_{\mathrm{f}}\delta_{4J}E_1^{(0)\mathrm{c}}\right)\left(a^2X(z_\beta) - \frac{3}{2}a^2z_\beta + z_\beta^3 - z_\beta^2X(z_\beta)\right)\Bigg\}. \end{aligned} \tag{57}$$

Taking the derivative of $f_{\beta 1}(z_\beta)$ with respect to z_β results in

$$\begin{aligned} f'_{\beta 1}(z_\beta) = \frac{b_{\beta J}^{-1}}{a^2}\Bigg\{ &-\frac{\epsilon_{\mathrm{f}}\delta_{4J}}{\pi \mathrm{i}A_1X(z_\beta)}\left[(A_2+A_3)\left(z_\beta^2X(z_\beta) - z_\beta^3 + \frac{a^2z_\beta}{2}\right) - a^2\left(\frac{A_2}{3}+\frac{A_3}{2}\right)(X(z_\beta)-z_\beta)\right] \\ &-\frac{1}{2}\mathrm{Re}\left[\sum_\alpha \mathrm{i}b_{J\alpha}p_\alpha U_\alpha\right]\left(z_\beta^2 - \frac{z_\beta^3}{X(z_\beta)} + \frac{5a^2z_\beta}{6X(z_\beta)} - \frac{a^2}{3}\right) \\ &-\frac{\mathrm{i}}{2}\left(\epsilon_{\mathrm{f}}\delta_{4J}E_1^{(0)\mathrm{c}} + \mathrm{Re}\left[\sum_\alpha b_{J\alpha}p_\alpha V_\alpha\right]\right)\left(z_\beta^2X(z_\beta) - z_\beta^2 + \frac{a^2}{2}\right)\Bigg\}. \end{aligned} \tag{58}$$

Since, to the author's knowledge, no similar analytical analysis has been carried out before for the non-ideal perturbed piezoelectric crack while considering the dielectric inside the crack, we prove the correctness of the solution by directly substituting Eq. (57) back into the Eqs. (20), (22) and (23). We find that the crack face and remote loading boundary conditions and the single-value condition of the displacement are all satisfied.

Employing Eq. (57) together with Eq. (3), the first order solution for displacement field can be obtained as

$$u_J^{(1)}(r,\theta) = 2\mathrm{Re}\sum_\beta a_{J\beta}b_{\beta K}^{-1}\Bigg\{-\frac{\epsilon_f\delta_{4K}}{\pi i A_1}\left[-\frac{A_3 a}{6}+\left(\frac{2A_2}{3}+\frac{A_3}{2}\right)r\Theta_\beta-\frac{A_2}{6}\sqrt{2ar\Theta_\beta}\right] - \frac{1}{6}\mathrm{Re}\left[\sum_\alpha \mathrm{i}b_{K\alpha}p_\alpha U_\alpha\right]\left[2r\Theta_\beta-\frac{1}{2}\sqrt{2ar\Theta_\beta}\right] + \frac{\mathrm{i}}{6}\left(\mathrm{Re}\left[\sum_\alpha b_{K\alpha}p_\alpha V_\alpha\right]+\epsilon_f\delta_{4K}E_1^{(0)c}\right)\left[-\frac{a}{2}+\frac{3r}{2}\Theta_\beta\right]\Bigg\} + O\left(r^{3/2}\right). \tag{59}$$

With Eqs. (58) and (11) the first order solution for generalized stress is given by

$$\Sigma_{2J}^{(1)}(r,\theta) = \frac{\sqrt{a}}{6\sqrt{2r}}\mathrm{Re}\left[\sum_\beta \frac{b_{J\beta}b_{\beta L}^{-1}}{\sqrt{\Theta_\beta}}\left(\mathrm{Re}\left[\sum_\alpha \mathrm{i}b_{L\alpha}p_\alpha U_\alpha\right]-\frac{\delta_{4L}H_{4K}}{H_{44}}\mathrm{Re}\left[\sum_\alpha \mathrm{i}b_{K\alpha}p_\alpha U_\alpha\right]\right)\right] - \frac{2\delta_{4J}\epsilon_f}{\pi i A_1}\left(\frac{2A_2}{3}+\frac{A_3}{2}\right)-\frac{2}{3}\mathrm{Re}\left[\sum_\alpha \mathrm{i}b_{J\alpha}p_\alpha U_\alpha\right]+O\left(\sqrt{r}\right). \tag{60}$$

The singular term of Eq. (60) on the x-axis in front of the right crack tip is

$$\Sigma_{2J\,\mathrm{singular}}^{(1)}(r,0) = \frac{\sqrt{a}\mathrm{Re}\left[\sum_\alpha \mathrm{i}b_{J\alpha}p_\alpha U_\alpha\right]}{6\sqrt{2r}} - \frac{\delta_{4J}H_{4K}}{H_{44}}\frac{\sqrt{a}\mathrm{Re}\left[\sum_\alpha \mathrm{i}b_{K\alpha}p_\alpha U_\alpha\right]}{6\sqrt{2r}}. \tag{61}$$

Hence the first order perturbation SEIFs are given by

$$\begin{cases} K_1^{(1)} = \frac{\sqrt{\pi a}}{6}\mathrm{Re}\left[\sum_\alpha \mathrm{i}b_{2\alpha}p_\alpha U_\alpha\right], & K_2^{(1)} = \frac{\sqrt{\pi a}}{6}\mathrm{Re}\left[\sum_\alpha \mathrm{i}b_{1\alpha}p_\alpha U_\alpha\right], \\ K_3^{(1)} = \frac{\sqrt{\pi a}}{6}\mathrm{Re}\left[\sum_\alpha \mathrm{i}b_{3\alpha}p_\alpha U_\alpha\right], & K_4^{(1)} = -\frac{\sqrt{\pi a}H_{4j}}{6H_{44}}\mathrm{Re}\left[\sum_\alpha \mathrm{i}b_{j\alpha}p_\alpha U_\alpha\right]. \end{cases} \tag{62}$$

Noticing Eq. (32), we can see $K_1^{(1)}$ is identically vanishing, i.e. the remote electro-mechanical loading cannot affect the mode I stress intensity to the first order of accuracy. For a transversely isotropic piezoelectric material with poling axis directed along the x_2-axis, we have $H_{41} = H_{43} = 0$ (Wang and Han, 1999), and together with Eqs. (32) and (38), one obtains $K_4^{(1)} = 0$. So the first order EIF is not influenced by the remote electro-mechanical loading either for a transversely isotropic piezoelectric material. However, for general piezoelectric material, the first order EIF may be influenced by the mechanical loading. Eq. (62) also suggests that the lateral stress σ_{11}^∞, σ_{13}^∞ and the electric loading at infinity cannot affect the intensity factors up to the first order of accuracy. And the stress and electric distributions of the first order solution have the same singularity but different angular distributions with the zeroth order solution. All intensity factors to the first order of accuracy are only related to the matrix material properties.

For isotropic materials, Kuang (1979) obtained an exact solution for a lip-flaw crack. When the height of flaw is small, it can be deduced that σ_{1j}^∞ and σ_{2j}^∞ cannot influence K_1 to the first order of accuracy. It is the same for a symmetric and non-symmetric regularly perturbed crack face (Wu, 1982, 1994). In Appendix B, by neglecting the electric components, Eq. (62) can be used to find the degenerate solution for isotropic materials, which is the same as Wu (1982). When the perturbation of the crack configuration is symmetric and materials are the same as Chen and Hsu (1997), the first order SIFs are all vanishing for anisotropic materials, i.e. σ_{1j}^∞ cannot influence the first order intensity factors. More efforts are needed to investigate whether the lateral stress and electric loading can effect the first order intensity factors for non-symmetric perturbed crack configuration.

Combining the second term of Eq. (45) and Eq. (58), one gets

$$\mathrm{Re}[g_1(x)] = \frac{1}{4}\left(\Pi_1\frac{x^3}{a^2}+\Pi_2 x\right), \tag{63}$$

where

$$\Pi_1 = 2\mathrm{Re}[M_{4J}]\left[-\frac{2\epsilon_f\delta_{4J}}{3\pi \mathrm{i} A_1}(A_2+A_3) - \frac{1}{3}\mathrm{Re}\left[\sum_\alpha \mathrm{i} b_{J\alpha}p_\alpha U_\alpha\right]\right] + \frac{H_{4J}}{3}\left(\mathrm{Re}\left[\sum_\alpha b_{J\alpha}p_\alpha V_\alpha\right] + \epsilon_f\delta_{4J}E_1^{(0)c}\right) - \frac{2}{3}\mathrm{Im}\left[\sum_\alpha a_{4\alpha}p_\alpha U_\alpha\right], \tag{64}$$

$$\Pi_2 = 2\mathrm{Re}[M_{4J}]\left[\frac{2\epsilon_f\delta_{4J}}{\pi \mathrm{i} A_1}\left(\frac{A_2}{3}+\frac{A_3}{2}\right) + \frac{1}{3}\mathrm{Re}\left[\sum_\alpha \mathrm{i} b_{J\alpha}p_\alpha U_\alpha\right]\right] - \frac{H_{4J}}{2}\left(\mathrm{Re}\left[\sum_\alpha b_{J\alpha}p_\alpha V_\alpha\right] + \epsilon_f\delta_{4J}E_1^{(0)c}\right) + \frac{2}{3}\mathrm{Im}\left[\sum_\alpha a_{4\alpha}p_\alpha U_\alpha\right]. \tag{65}$$

Substituting Eqs. (56) and (63) into the first term of Eq. (13) and the third term of Eq. (13) respectively, the structure of electric field of the first order perturbation inside the crack on x-axis can be given by

$$\begin{cases} E_1^{(1)c}(x,0) = -2\mathrm{Re}\left[g_1'(x)\right] = -\frac{1}{2}\left(3\Pi_1\frac{x^2}{a^2} + \Pi_2\right), \\ E_2^{(1)c}(x,0) = 2\mathrm{Im}\left[g_1'(x)\right] = -\frac{1}{\pi \mathrm{i} A_1}\left[(A_2+A_3)\frac{x^2}{a^2} - \left(\frac{A_3}{2}+\frac{A_2}{3}\right)\right]. \end{cases} \tag{66}$$

The electric distribution of the first order solution is non-homogeneous inside the crack, which is different from that of the usual permeable ideal crack. The effect of this inhomogeneous electric distribution becomes apparent when the perturbation to the crack configuration becomes large. From Eqs. (12), (17) and (13), the electric potential jump between the upper and lower face of non-ideal crack can be shown as

$$\phi(x, Y_+(x)) - \phi(x, Y_-(x)) = -2\varepsilon(Y_+(x) - Y_-(x))E_2^{(0)c}. \tag{67}$$

It is easy to get

$$2\varepsilon D_2^{(0)c}(Y_+(x) - Y_-(x)) = \epsilon_f(\phi(x, Y_-(x)) - \phi(x, Y_+(x))), \tag{68}$$

which coincides with the theory of a discontinuous surface of electric potential. Based on this fact, Hao and Shen (1994) proposed an electric boundary condition as $D_2^+ = D_2^-$, $D_2^+(u_2^+ - u_2^-) = \epsilon_f(\phi^- - \phi^+)$ for the ideal permeable crack, where $u_J^+ - u_J^-$ are the generalized opening displacements between the opposing crack faces.

6. Energy release rate for the permeable non-ideal crack

The energy release rate precise to the order of ε can be obtained by the closure integral

$$G = \frac{1}{2l}\int_0^l \Sigma_{2J}(l-r)\Delta_J(r)\mathrm{d}r, \tag{69}$$

where l is an infinitesimal length and the generalized displacement jump on the crack face can be written as

$$\Delta_J(x) = u_J^+(x) - u_J^-(x) = (u_J^{(0)+} - u_J^{(0)-}) + \varepsilon(u_J^{(1)+} - u_J^{(1)-}) + O(\varepsilon^2). \tag{70}$$

Invoking Eqs. (44) and (59) and neglecting the terms with orders higher than $\sqrt{r}$, we can get,

$$\Delta_{J0} = u_J^{(0)+}(x) - u_J^{(0)-}(x) = \sqrt{2ar}\left\{H_{jk}\Sigma_{2k}^\infty - H_{j4}H_{4k}\Sigma_{2k}^\infty/H_{44}, 0\right\}, \tag{71}$$

$$\Delta_{J1} = u_J^{(1)+}(x) - u_J^{(1)-}(x) = \frac{\sqrt{2ar}}{6}\left\{H_{jk}\mathrm{Re}\left[\sum_\alpha \mathrm{i}b_{k\alpha}p_\alpha U_\alpha\right] - H_{j4}H_{4k}\mathrm{Re}\left[\sum_\alpha \mathrm{i}b_{k\alpha}p_\alpha U_\alpha\right]\Big/ H_{44}, 0\right\}. \tag{72}$$

With Eqs. (42), (61), (69) and (70), we get the energy release rate to the first order accuracy,

$$G = \frac{1}{4}[H_{ij}k_i^{(0)}k_j^{(0)} - H_{44}k_4^{(0)^2} + \frac{\varepsilon}{3}(H_{ij}k_i^{(0)}k_j^{(1)} - H_{44}k_4^{(0)}k_4^{(1)})]. \tag{73}$$

where

$$\mathbf{k}^{(\alpha)} = \{K_2^{(\alpha)}, K_1^{(\alpha)}, K_3^{(\alpha)}, K_4^{(\alpha)}\}, \quad \alpha = 0, 1.$$

The zeroth order energy release rate is identical with Wang and Han (1999). The above result manifests that energy release rate does not depend on the electric loading at infinity. This is an unsolved problem (Park and Sun, 1995; Lynch, 1998). One way to solve this difficulty seems to require a more appropriate model such as a non-linear piezoelectric constitutive relationship, e.g. the domain switching effect to be considered.

7. Results for impermeable and conducting non-ideal crack

The above sections mainly deal with a permeable non-ideal crack using the exact electric boundary condition. For the completeness of the paper, the impermeable and conducting electric boundary conditions are also presented. In this section we will give respectively the generalized SIFs and the energy release rate for the impermeable and conducting non-ideal crack with the crack configuration defined by Eq. (50).

For an impermeable non-ideal crack, the boundary condition (18) will be slightly modified by letting the right-hand side of the second term of Eq. (18) equal zero and abnegating the third term of Eq. (18). For the zeroth order solution, the third term of Eq. (19) is waived and the right-hand side of the second term of Eq. (19) equals zero, and the remote boundary condition remains intact. The solving process becomes much more simplified since in Eq. (29) the singular integral term containing an unknown function does not exist any longer. It is easy to show that the generalized SIF can be given by (Suo et al., 1992)

$$\begin{cases} K_1^{(0)} = \sqrt{\pi a}\sigma_{22}^\infty, & K_2^{(0)} = \sqrt{\pi a}\sigma_{21}^\infty, \\ K_3^{(0)} = \sqrt{\pi a}\sigma_{23}^\infty, & K_4^{(0)} = \sqrt{\pi a}D_2^\infty. \end{cases} \tag{74}$$

For the first order solution, the term containing ϵ_f in Eq. (52) is discarded, hence with the availability of Eq. (52), the first order solution is solved. The generalized stress intensity of the first order is,

$$\begin{cases} K_1^{(1)} = \frac{\sqrt{\pi a}}{6}\mathrm{Re}\left[\sum_\alpha \mathrm{i}b_{2\alpha}p_\alpha U_\alpha\right], & K_2^{(1)} = \frac{\sqrt{\pi a}}{6}\mathrm{Re}\left[\sum_\alpha \mathrm{i}b_{1\alpha}p_\alpha U_\alpha\right], \\ K_3^{(1)} = \frac{\sqrt{\pi a}}{6}\mathrm{Re}\left[\sum_\alpha \mathrm{i}b_{3\alpha}p_\alpha U_\alpha\right], & K_4^{(1)} = \frac{\sqrt{\pi a}}{6}\mathrm{Re}\left[\sum_\alpha \mathrm{i}b_{4\alpha}p_\alpha U_\alpha\right], \end{cases} \tag{75}$$

where

$$U_\alpha = b_{\alpha J}^{-1}\Sigma_{2J}^\infty \tag{76}$$

Similarly to that of the permeable crack, Σ_{2J}^∞ cannot influence $K_1^{(1)}$. We can also obtain the energy release rate to the first order of accuracy for impermeable non-ideal crack,

$$G = \frac{1}{4}\left(H_{IJ}k_I^{(0)}k_J^{(0)} + \frac{\varepsilon}{3}H_{IJ}k_I^{(0)}k_J^{(1)}\right). \tag{77}$$

For a conducting crack, the second terms of Eqs. (18)–(20) will be abandoned. We take the reference electric potential on the crack faces as the zero, so that the right-hand side of the third terms of Eqs.

(18)–(20) equal zero. Hence an analogy can be made between a conducting crack and an impermeable crack for finding the intensity factors. We define

$$\hat{a}_{J\alpha} = \begin{cases} a_{j\alpha} & J = 1,2,3, \\ -b_{4\alpha} & J = 4, \end{cases} \qquad \hat{b}_{J\alpha} = \begin{cases} b_{j\alpha} & J = 1,2,3, \\ -a_{4\alpha} & J = 4, \end{cases}$$

so

$$\begin{aligned} \hat{\Sigma}_{2J}(z) &= \begin{Bmatrix} \sigma_{2j} \\ E_1 \end{Bmatrix} = 2\mathrm{Re}\left[\sum_{\alpha=1}^{4} \hat{b}_{J\alpha} f'_\alpha(z_\alpha)\right], \\ \hat{\Sigma}_{1J}(z) &= \begin{Bmatrix} \sigma_{1j} \\ -E_2 \end{Bmatrix} = -2\mathrm{Re}\left[\sum_{\alpha=1}^{4} \hat{b}_{J\alpha} p_\alpha f'_\alpha(z_\alpha)\right], \end{aligned} \tag{78}$$

and

$$\hat{u}_J(z) = \begin{Bmatrix} u_j \\ \hat{u}_4 \end{Bmatrix} = 2\mathrm{Re}\sum_{\alpha=1}^{4} \hat{a}_{J\alpha} f_\alpha(z_\alpha), \tag{79}$$

where $\hat{u}_4$ is the total flux of electric displacement normal to a curve. The SEIFs for the zeroth order solution are (Suo 1993)

$$\begin{cases} \hat{K}_1^{(0)} = \sqrt{\pi a}\sigma_{22}^\infty, & \hat{K}_2^{(0)} = \sqrt{\pi a}\sigma_{21}^\infty, \\ \hat{K}_3^{(0)} = \sqrt{\pi a}\sigma_{23}^\infty, & \hat{K}_4^{(0)} = \sqrt{\pi a}E_1^\infty. \end{cases} \tag{80}$$

and the first order solution can also be derived as follows,

$$\begin{cases} \hat{K}_1^{(1)} = \frac{\sqrt{\pi a}}{6}\mathrm{Re}\left[\sum_\alpha \mathrm{i}\hat{b}_{2\alpha} p_\alpha \hat{U}_\alpha\right], & \hat{K}_2^{(1)} = \frac{\sqrt{\pi a}}{6}\mathrm{Re}\left[\sum_\alpha \mathrm{i}\hat{b}_{1\alpha} p_\alpha \hat{U}_\alpha\right], \\ \hat{K}_3^{(1)} = \frac{\sqrt{\pi a}}{6}\mathrm{Re}\left[\sum_\alpha \mathrm{i}\hat{b}_{3\alpha} p_\alpha \hat{U}_\alpha\right], & \hat{K}_4^{(1)} = \frac{\sqrt{\pi a}}{6}\mathrm{Re}\left[\sum_\alpha \mathrm{i}\hat{b}_{4\alpha} p_\alpha \hat{U}_\alpha\right]. \end{cases} \tag{81}$$

where

$$\hat{U}_\alpha = \hat{b}_{\alpha J}^{-1} \hat{\Sigma}_{2J}^\infty. \tag{82}$$

Is $\hat{K}_1^{(1)}$ equal to zero now like those for permeable and impermeable crack for all piezoelectric materials? Researches on the properties of the $\hat{\mathbf{B}}\mathbf{P}\hat{\mathbf{B}}^{-1}$ may be helpful to answer this question. The energy release rate for conducting crack is

$$\hat{G} = \frac{1}{4}\left(\hat{H}_{IJ}\hat{k}_I^{(0)}\hat{k}_J^{(0)} + \frac{\varepsilon}{3}\hat{H}_{IJ}\hat{k}_I^{(0)}\hat{k}_J^{(1)}\right), \tag{83}$$

where

$$\hat{H}_{IJ} = \mathrm{i}\left(\sum_{\alpha=1}^{4}\left(\hat{a}_{K\alpha}\hat{b}_{\alpha J}^{-1} - \bar{\hat{a}}_{K\alpha}\bar{\hat{b}}_{\alpha J}^{-1}\right)\right), \tag{84}$$

which is formally as that of an impermeable crack.

8. Numerical example for the permeable crack boundary condition and discussions

In this section we present numerical form of the present solution. For a transversely isotropic piezoelectrics with the poling axis directed along the x_2-axis, the matrices **Q**, **R**, **T** are:

$$\mathbf{Q}=\begin{bmatrix} c_{11} & 0 & 0 & 0 \\ 0 & c_{44} & 0 & e_{15} \\ 0 & 0 & \frac{c_{11}-c_{22}}{2} & 0 \\ 0 & e_{15} & 0 & -\kappa_{11} \end{bmatrix}, \quad \mathbf{R}=\begin{bmatrix} 0 & c_{13} & 0 & e_{31} \\ c_{44} & 0 & 0 & 0 \\ 0 & 0 & 0 & 0 \\ e_{15} & 0 & 0 & 0 \end{bmatrix}, \quad \mathbf{T}=\begin{bmatrix} c_{44} & 0 & 0 & 0 \\ 0 & c_{33} & 0 & e_{33} \\ 0 & 0 & c_{44} & 0 \\ 0 & e_{33} & 0 & -\kappa_{33} \end{bmatrix}.$$

It should be noted that all material constants in the **Q**, **R**, **T** matrices are measured in the material coordinate system where the poling direction is parallel to the x_3-axis. The material constants for the dielectric inside the crack and PZT-4 whose poling axis is along the x_3-axis are listed as follows (Park and Sun, 1995):

$$\begin{aligned} &\epsilon_f = 8.85\times10^{-12}\ \left(\mathrm{C^2\,N^{-1}\,m^{-2}}\right) \\ &c_{11}=139,\quad c_{33}=113,\quad c_{12}=77.8,\quad c_{13}=74.3,\quad c_{44}=25.6\ (\mathrm{GPa}), \\ &e_{33}=13.8,\quad e_{31}=-6.98,\quad e_{15}=13.4\ \left(\mathrm{C\,m^{-2}}\right), \\ &\kappa_{11}=6.00\times10^{-9},\quad \kappa_{33}=5.47\times10^{-9}\ \left(\mathrm{C^2\,N^{-1}\,m^{-2}}\right) \end{aligned}$$

Using a symbolic manipulator such as Mathematica™ or Maple™, it is quite easy to get the SEIFs and energy release rate from the first term of Eq. (38), Eqs. (43), (62) and (73). To the first order of accuracy, we have $K_J = K_J^{(0)} + \varepsilon K_J^{(1)}$ and $G = G_1^{(0)} + \varepsilon G_1^{(1)}$ and they are,

$$\begin{aligned} K_1 &= \sqrt{\pi a}\sigma_{22}^{\infty} + O(\varepsilon^2)\ \left(\mathrm{Pa\,m^{1/2}}\right), \\ K_2 &= (1-0.3706\varepsilon)\sqrt{\pi a}\sigma_{12}^{\infty} + O(\varepsilon^2)\ \left(\mathrm{Pa\,m^{1/2}}\right), \\ K_3 &= (1-0.1822\varepsilon)\sqrt{\pi a}\sigma_{23}^{\infty} + O(\varepsilon^2)\ \left(\mathrm{Pa\,m^{1/2}}\right), \\ K_4 &= 0.2533\times10^{-9}\sqrt{\pi a}\sigma_{22}^{\infty} + O(\varepsilon^2)\ \left(\mathrm{C\,m^{-3/2}}\right), \end{aligned} \tag{85}$$

$$G = \pi a\left[1.155\sigma_{22}^{\infty 2} + (0.881-0.1088\varepsilon)\sigma_{12}^{\infty 2} + (1.786-0.1085\varepsilon)\sigma_{23}^{\infty 2}\right]\times10^{-11} + O(\varepsilon^2)\ (\mathrm{N/m}). \tag{86}$$

When the perturbation is of an order of 10^{-2}, the influence order by the perturbation is of 10^{-3} for mode II and mode III intensity factors and the energy release rate and there is no effect on K_1 and K_4. The perturbation effect on the electro-mechanical field inside the matrix is small. However it does not suggest that the contact permeable electric boundary condition is appropriate to model this non-ideal perturbed crack configuration due to that the internal electric field in the crack is very large which will be shown latter. Fig. 2 shows the comparison of the critical mechanical loads of the permeable model with the impermeable model where the half crack length is 1 cm, and the critical extended energy release rate $G_{cr} = 1.44$ N/m (Fulton and Gao, 1997). It is shown that the critical stress for the permeable mode is invariant and is lower than the impermeable model.

To study the piezoelectric effects on the SEIFs, we suppose a material with the same elastic and dielectric material properties but the piezoelectric constants λ times those of the PZT-4. By varying the piezoelectric constant ratio λ, Fig. 3a and b show the variations of SEIFs with respect to λ. Since the out-of-plane stress component σ_{23} is independent of the piezoelectric constants for transversely isotropic materials, so is K_3. The value of K_3 is the same as PZT-4 and it will not be given. The zeroth SIFs are the same as those of the isotropic case, so they will not be plotted either. From Fig. 3a, we can see the first order mode II SIF decreases as λ increases and the decrease effect approaches a constant value as λ becomes large enough. In Fig. 3b, the EIF increases almost in a linear manner as λ increases, which means the larger the piezoelectric effect the bigger the EIF. When $\lambda = 0$, i.e. there is no piezoelectric effect, the remote electro-mechanical loading cannot induce any EIF at all. The first order perturbation effect is also small for the isolating model, and the first order SEIFs are plotted in Appendix C (Fig. 5a and b).

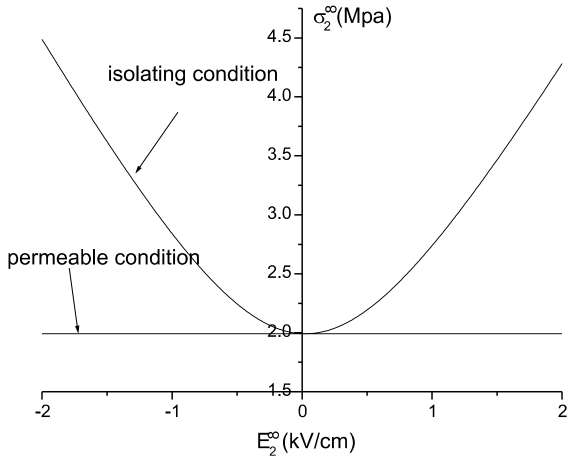

Fig. 2. Critical stresses for the isolating and permeable electric boundary condition under different electric loading.

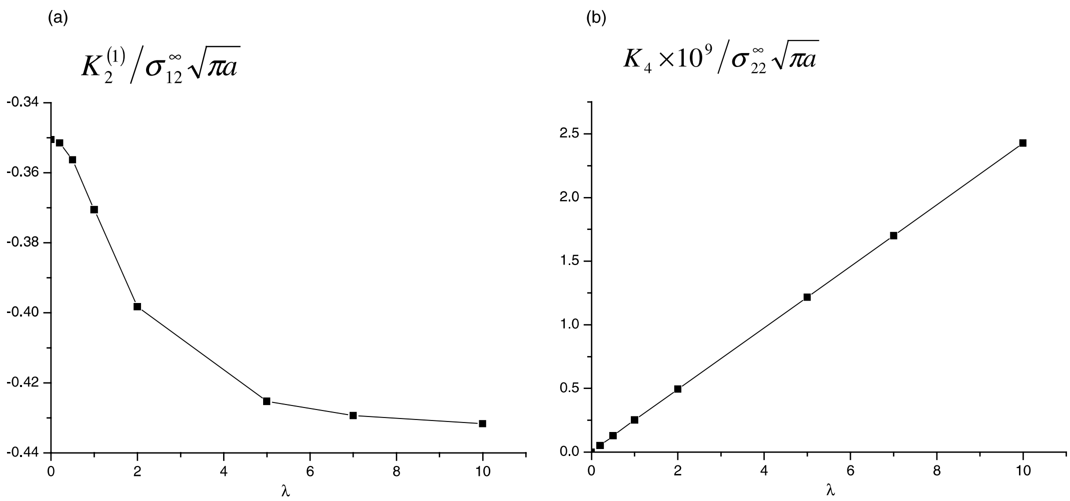

Fig. 3. (a) The variation of the first order dimensionless mode II SIF $K_2^{(1)}/\sigma_{12}^\infty\sqrt{\pi a}$ with respect to the piezoelectric constant material ratio λ under the permeable boundary condition and (b) the variation of the dimensionless EIF $K_4\times 10^9/\sigma_{12}^\infty\sqrt{\pi a}$ with respect to the piezoelectric constant material ratio λ under the permeable boundary condition.

In practice an application of remote electric displacement loading is usually not achievable, we give the internal electric field in terms of the remote electro-mechanical loading. Knowing Eq. (37), it is not difficult to show that

$$\begin{aligned} D_1^\infty &= 1.306\times 10^{-8}E_1^\infty + 5.25\times 10^{-10}\sigma_{12}^\infty\ \left(\mathrm{C/m^2}\right),\\ D_2^\infty &= 1.003\times 10^{-8}E_2^\infty - 1.783\times 10^{-10}\sigma_{11}^\infty + 2.398\times 10^{-10}\sigma_{22}^\infty\ \left(\mathrm{C/m^2}\right). \end{aligned} \tag{87}$$

With Eqs. (40), (66), (55), (64), (65) and (87), we obtained the zeroth and first order electric field solutions inside the crack as

$$
\begin{aligned}
E_1^{(0)c} &= E_1^\infty - 2.140 \times 10^{-2}\sigma_{22}^\infty + 4.021 \times 10^{-2}\sigma_{12}^\infty \ (\mathrm{V/m}),\\
E_2^{(0)c} &= 1133.8E_2^\infty - 20.16\sigma_{11}^\infty - 1.526\sigma_{22}^\infty \ (\mathrm{V/m}),
\end{aligned} \tag{88}
$$

$$
\begin{aligned}
E_1^{(1)c}(x,0) &= \left(9.483 \times 10^{-2}\sigma_{12}^\infty - 1.141E_1^\infty\right)x^2/a^2 + 0.5704E_1^\infty - 2.806 \times 10^{-2}\sigma_{12}^\infty,\\
E_2^{(1)c}(x,0) &= \left(2.928 \times 10^6 E_2^\infty - 5.208 \times 10^4\sigma_{11}^\infty - 3.906 \times 10^3\sigma_{22}^\infty\right)x^2/a^2\\
&\quad - 9.763 \times 10^5 E_2^\infty + 1.737 \times 10^4\sigma_{11}^\infty + 1.291 \times 10^3\sigma_{22}^\infty \ (\mathrm{V/m}).
\end{aligned} \tag{89}
$$

It can be seen from Eq. (88) that the first order perturbation for the E_2 cannot be neglected even for an order of a 10^{-3} scale perturbation of the crack configuration. Plotted in Fig. 4 are the zeroth order and the total internal electric field distributions when the matrix is subjected to a mechanical loading $\sigma_{22}^\infty = 1$ Mpa with different remote electric loading. It can be seen that when the perturbation becomes large, the internal electric field is significantly magnified near the crack tip. Since the gap of the perturbed crack in the middle of the crack is larger, from a physical qualitative view, the electric field is difficult to permeate and consequently electric flux lines inside the crack becomes very dense near the crack tip for easier penetration of the electric field there. For $\varepsilon = 0.03$, i.e. the half height of crack is $1/100$ of the half length of the crack, the internal electric field near the crack tip is of order 10^4 MV/m which is too high to sustain for general dielectrics. Since the dielectric inside the crack is usually air or silicon oil with a relatively low breakdown strength, it is very likely that the breakdown of the dielectric within the crack takes place before the matrix does, so the conducting electric boundary condition near the tip should be considered. Although the present permeable model does not predict the influence of the remote electric loading on the fracture toughness as indicated by Park and Sun (1995) and Lynch (1998), it suggests that the electric boundary condition inside near the crack tip needs further investigation if it breaks down. The present model indicates that a conducting electric boundary condition near the crack tip and an isolating electric boundary condition in the middle may be a suitable model for the piezoelectric fracture problems. Researches on this crack boundary condition are underway.

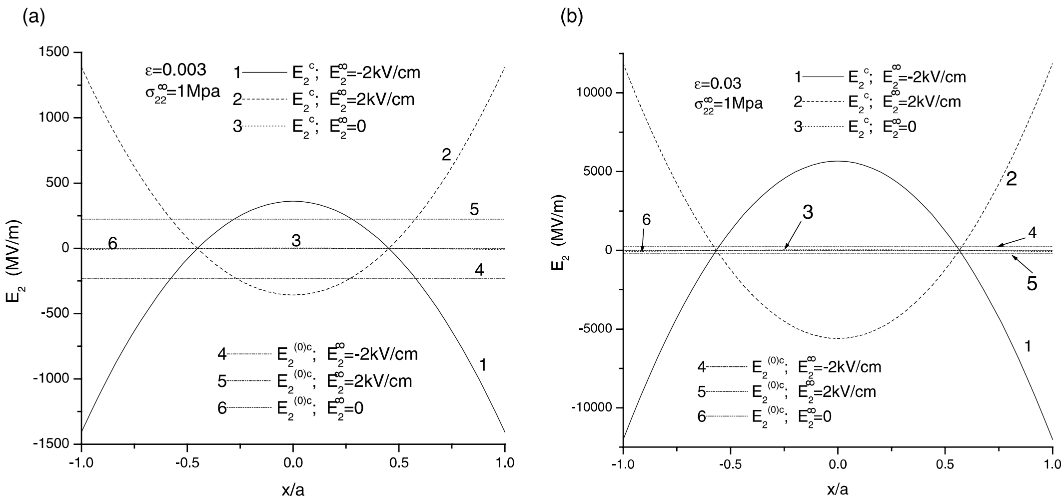

Fig. 4. (a) Electric field distribution inside the crack when the perturbation is $\varepsilon = 0.003$ and the remote mechanical loading $\sigma_{22}^\infty = 1$ MPa under the permeable boundary condition and (b) electric field distribution inside the crack when the perturbation is $\varepsilon = 0.03$ and the remote mechanical loading $\sigma_{22}^\infty = 1$ MPa under the permeable boundary condition.

9. Results and conclusions

In this paper an infinite piezoelectric plate with a centered symmetrically perturbed non-ideal crack for three possible electric boundary conditions are discussed. From this study some results and conclusions are obtained:

(1) The asymptotic stress and displacement fields to the first order of accuracy near the crack tip are given. The results show that the first order solutions have the same singularity in r, but different angular distributions with the zeroth order solutions.

(2) The SEIFs to the first order of accuracy are given. It is found that the remote electric loading has no contribution to the SEIFs up to the first order of accuracy for the permeable non-ideal crack. But the zeroth order SEIFs for the impermeable and conducting non-ideal crack are determined independently by the remote mechanical and electrical loading. For all three electric boundary conditions, the lateral stresses σ_{11}^{∞}, σ_{13}^{∞} have no contribution to the SEIFs to the first order of accuracy. For the permeable electric boundary condition, σ_{2j}^{∞} cannot affect the first order mode I SIF. For an asymmetrical non-ideal crack the remote lateral stress σ_{11}^{∞}, σ_{13}^{∞} and electric displacement D_1^{∞} may have contribution to the SEIFs as can be seen from Eq. (50), but its closed solution may be very complex, so as a first approximation, we only address a symmetrically perturbed non-ideal crack. Whether the lateral stresses and electric displacement can come into effect for the non-symmetric perturbed crack needs further investigation. The electric loading D_1^{∞} for the impermeable crack and E_2^{∞} for the conducting crack cannot affect the zeroth and the first order SEIFs but the electric loading D_2^{∞} and E_1^{∞} for the impermeable and conducting model respectively have contribution to both the zeroth and the first order SEIFs.

(3) For the permeable electric boundary condition, the quadratic electric field distribution for the first order solution inside the crack is different from the ideal crack in which the electric field distribution is homogeneous. The perturbation has a slight effect on the intensity factors and the energy release rate. However, when the perturbation is even of an order of 10^{-3}, its influence on the electric distribution inside the crack is of the same order as its zeroth order solution. When the perturbation becomes larger, the electric field concentration effect inside the crack probably causes the dielectric inside the crack to break down before the matrix does. Hence the permeable electric boundary condition fails and the present model suggests that a conducting electric boundary condition near the crack tip and an isolating electric in the middle may be a suitable model for a real crack.

Acknowledgements

This work is supported by the National Science Foundation of China through the Grant 10072033. Helpful suggestions by the reviewers are gratefully acknowledged.

Appendix A. Some singular definite integrals

Following Muskhelishvili (1953), we list several singular integrals used in the paper.

$$\begin{cases} \int_{-a}^{a} \frac{t}{(t-z)X^+(t)}\mathrm{d}t = \pi\mathrm{i}\left(\frac{z}{X(z)} - 1\right), \\ \int_{-a}^{a} \frac{t}{(t-x)X^+(t)}\mathrm{d}t = -\pi\mathrm{i}, \end{cases} \qquad \begin{cases} \int_{-a}^{a} \frac{t^3}{(t-z)X^+(t)}\mathrm{d}t = \pi\mathrm{i}\left(\frac{z^3}{X(z)} - z^2 - \frac{a^2}{2}\right), \\ \int_{-a}^{a} \frac{t^3}{(t-x)X^+(t)}\mathrm{d}t = -\pi\mathrm{i}(x^2 + a^2/2), \end{cases},$$

$$\begin{cases} \int_{-a}^{a} \frac{X^+(t)}{t-z}\mathrm{d}t = \pi\mathrm{i}[X(z) - z], \\ \int_{-a}^{a} \frac{X^+(t)}{t-x}\mathrm{d}t = -\pi\mathrm{i}x, \end{cases} \qquad \begin{cases} \int_{-a}^{a} \frac{tX^+(t)}{t-z}\mathrm{d}t = \pi\mathrm{i}[zX(z) - z^2 + a^2/2], \\ \int_{-a}^{a} \frac{tX^+(t)}{t-x}\mathrm{d}t = \pi\mathrm{i}(-x^2 + a^2/2), \end{cases}$$

$$\begin{cases} \int_{-a}^{a} \frac{t^2X^+(t)}{t-z}\,\mathrm{d}t = \pi \mathrm{i}[z^2X(z) - z^3 + a^2z/2] \\ \int_{-a}^{a} \frac{t^2X^+(t)}{t-x}\,\mathrm{d}t = \pi \mathrm{i}(-x^3 + a^2x/2) \end{cases}$$

Appendix B. The SIFs for isotropic elastic materials using the obtained solution

The zeroth order SIFs are obviously identical to those of isotropic material. To obtain the first the order SIFs, by neglecting the electric component in the obtained solution (60), the stress distribution directly in front of the crack tip is

$$\sigma^{(1)}_{2j\,\mathrm{singular}}(r,0) = \frac{\sigma^{\infty}_{2k}\sqrt{a}}{6\sqrt{2r}}\mathrm{Re}\left[\sum_{\alpha} \mathrm{i}b_{j\alpha}p_\alpha b^{-1}_{\alpha k}\right]. \tag{B.1}$$

Ting (1996) points out that the left side of Eq. (31) also holds no matter whether the material is degenerate or not. Since $\mathbf{N}_i$, **S, L** are all real matrixes, Eq. (B.1) can be rewritten as

$$\sigma^{(1)}_{2j\,\mathrm{singular}}(r,0) = \frac{\sigma^{\infty}_{2k}\sqrt{a}}{6\sqrt{2r}}(\mathbf{N}_3\mathbf{L}^{-1})_{jk}. \tag{B.2}$$

The explicit form of matrixes $\mathbf{N}_3$ and $\mathbf{L}$ for isotropic materials can be found in Ting's book (1996) as

$$\mathbf{N}_3 = \begin{bmatrix} -\frac{4\mu(\lambda+\mu)}{\lambda+2\mu} & 0 & 0 \\ 0 & 0 & 0 \\ 0 & 0 & -\mu \end{bmatrix}, \qquad \mathbf{L} = \begin{bmatrix} \frac{2\mu(\lambda+\mu)}{\lambda+2\mu} & 0 & 0 \\ 0 & \frac{2\mu(\lambda+\mu)}{\lambda+2\mu} & 0 \\ 0 & 0 & \mu \end{bmatrix},$$

where λ is the Lame constant and the μ shear modulus. After a matrix multiplication, one reaches

$$\mathbf{N}_3\mathbf{L}^{-1} = \begin{bmatrix} -2 & 0 & 0 \\ 0 & 0 & 0 \\ 0 & 0 & -1 \end{bmatrix},$$

which is irrespective of the material constants. Hence the first order perturbation SIFs are given by

$$K^{(1)}_1 = 0, \qquad K^{(1)}_2 = -\frac{\sqrt{\pi a}}{3}\sigma^{\infty}_{12}, \qquad K^{(1)}_3 = -\frac{\sqrt{\pi a}}{6}\sigma^{\infty}_{23},$$

which are identical to those of Wu (1982) after $K^{(1)}_2$ being corrected in his paper. This confirms the correctness of the present perturbation solution.

Appendix C. Variations of the first order SEIFs with respect to the piezoelectric constant ratio λ for the isolating model

The zeroth SIFs and the first order mode I SIF will not be plotted here for the same reason as stated for the permeable case. The numerical results find that the first order mode II SIF is the same as that of the permeable case (Fig. 3a). The remote electro-mechanical loading can influence the EIF to the first order of accuracy, however the effect of the mechanical loading is small compared to that of the electric loading (Fig. 5).

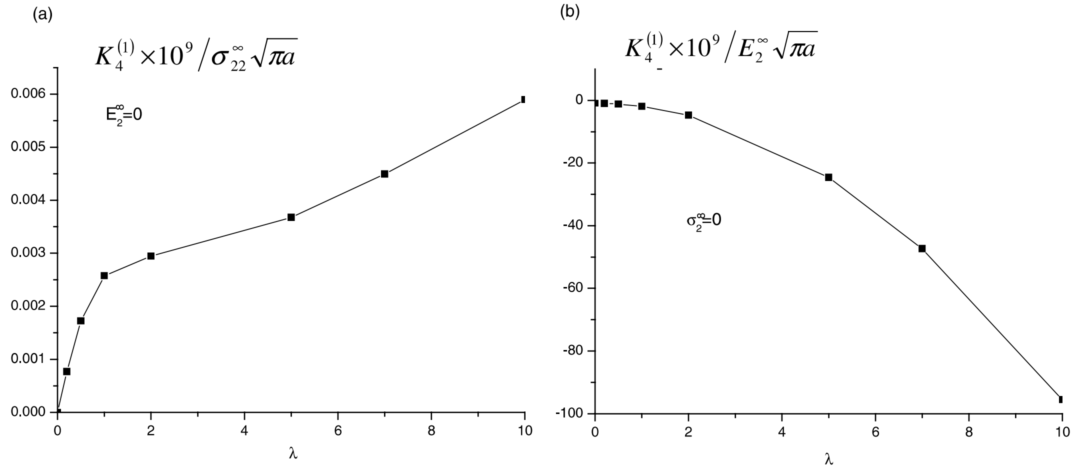

Fig. 5. (a) The variation of the first order dimensionless EIF $K_4^{(1)} \times 10^9/\sigma_{22}^{\infty}\sqrt{\pi a}$ with respect to the piezoelectric constant material ratio λ under the impermeable boundary condition and (b) the variation of the first order dimensionless EIF $K_4^{(1)} \times 10^9/\sigma_{22}^{\infty}\sqrt{\pi a}$ with respect to the piezoelectric constant material ratio λ under the impermeable boundary condition.

References

Chen, C.-H., Hsu, J., 1997. The stress intensity factors of regularly perturbed-interface cracks of anisotropic bimaterials. International Journal of Solids and Structures 34, 1235–1253.

Chung, M.Y., Ting, T.C.T., 1996. Piezoelectric solid with an elliptic inclusion or hole. International Journal of Solids and Structures 33, 3343–3461.

Deeg, W.F., 1980. The analysis of dislocation, crack and inclusion problems in piezoelectric solids. Ph.D. Thesis, Stanford University, CA.

Dunn, M.L., 1994. The effects of crack face boundary conditions on the fracture mechanics. Engineering Fracture Mechanics 48, 25–39.

Fulton, C.C., Gao, H., 1997. Electrical nonlinearity in fracture of piezoelectric ceramics. ASME Applied Mechanics Review 50, S56–S63.

Gao, C.-F., Fan, W.-X., 1999. Exact solutions for the plane problem in piezoelectric materials with an elliptic or a crack. International Journal of Solids and Structures 36, 2527–2540.

Gao, C.-F, Wang, M.-Z., 2000. Collinear permeable cracks between dissimilar piezoelectric materials. International Journal of Engineering Science 37, 4969–4986.

Hao, T.-H, Shen, Z.-Y., 1994. A new electric boundary condition of electric fracture mechanics and its applications. Engineering Fracture Mechanics 47, 793–802.

Irwin, G.R., 1957. Analysis of stresses and strains near the end of a crack traversing a plate. ASME Journal of Applied Mechanics 24, 361–364.

Kuang, Z.-B., 1979. Stress analysis for plane curved polygonal defects containing cusps only. Acta Mech Sinica 11, 118–128.

Kuang, Z.-B., Ma, F.-S., 2000. Fields Near Crack Tips. Xi'an Jiaotong University Press, Xi'an.

Lynch, C.L., 1998. Fracture of ferroelectric and relaxor electric-ceramics: influence of electric field. Acta Materialia 46, 599–608.

McMeeking, R.M., 1989. Electrostrictive stresses near crack-like flaws. Journal of Applied Mathematics and Physics 40, 615–627.

McMeeking, R.M., 1999. Crack tip energy release rate for a piezoelectric compact tension specimen. Engineering Fracture Mechanics 64, 217–244.

Muskhelishvili, N.I., 1953. Some Basic Problems of The Mathematical Theory of Elasticity. Noordhoff, Leyden.

Muskhelishvili, N.I., 1975. Singular Integral Equations. Noordhoff, Gronigen, Holland.

Pak, Y.E., 1990. Crack extension force in a piezoelectric material. ASME Journal of Applied Mechanics 57, 647–653.

Pak, Y.E., 1992. Linear electro-elastic fracture mechanics of piezoelectric materials. International Journal of Fracture 54, 79–100.

Park, S., Sun, C.T., 1995. Fracture criteria for piezoelectric materials. Journal of American Ceramic Society 78, 1475–1480.

Parton, V.Z., 1976. Fracture mechanics of piezoelectric materials. Acta Astronautica 3, 671–683.

Shen, S., Kuang, Z.-B., 1998. Interface crack in bi-piezothermoelectric media and the interaction with a point heat source. International Journal of Solids and Structures 35, 3899–3915.

Sosa, H.A., 1991. Plane problems in piezoelectric media with defects. International Journal of Solids and Structures 28, 491–505.

Sosa, H.A., Khutoryansky, N., 1996. New developments concerning piezoelectric materials with defects. International Journal of Solids and Structures 33, 3399–3414.

Suo, Z., 1990. Singularities interfaces and cracks in dissimilar anisotropic media. Proceeding of Royal Society (London) A427, 331–358.

Suo, Z., Kuo, C.M., Barnett, D.M., Willis, J.R., 1992. Fracture mechanics for piezoelectric ceramics. Journal of the Mechanics and Physics of Solids 40, 739–765.

Suo, Z., 1993. Models for breakdown-resistant dielectric and ferroelectric ceramics. Journal of the Mechanics and Physics of Solids 41, 1155–1176.

Ting, T.C.T., 1996. Anisotropic Elasticity and it's Application. Oxford University Press, London.

Wang, B., 1992. Three dimensional analysis of an ellipsoidal inclusion in piezoelectric material. International Journal of Solids and Structures 22, 965–983.

Wang, T.C., Han, X.L., 1999. Fracture mechanics of piezoelectric materials. International Journal of Fracture 98, 15–35.

Wu, C.H., 1982. Unconventional internal cracks part 1: symmetric variations of a straight crack. ASME Journal of Applied Mechanics 49, 62–68.

Wu, C.H., 1994. Regularly and singularly perturbed cracks. Quarterly Applied Mathematics 52, 529–543.

Zhang, T.-Y., Qian, C.-F., Tong, P., 1998. Linear electro-elastic analysis of a cavity or a crack in a piezoelectric material. International Journal of Solids and Structures 35, 2121–2149.